Journal of Engineering Research and Reports

21(1): 1-14, 2021; Article no.JERR.73935
ISSN: 2582-2926

Behavior of Self Compacted Concrete Ferrocement Beams

Abeer M. Erfan[1*], Tamer H. K. Elafandy[2], Mahmoud M. Mahran[1] and Mohamed Said[1]

[1]Department of Civil Engineering, Shoubra Faculty of Engineering/ Benha University, 108 Shoubra St., Shoubra, Cairo, Egypt.
[2]Department of Civil Engineering, Housing and Building Research Center (HBRC), Cairo, Egypt.

Authors' contributions

This work was carried out in collaboration among all authors. All authors read and approved the final manuscript.

Article Information

DOI: 10.9734/JERR/2021/v21i117434
Editor(s):
(1) Prof. Hamdy Mohy El-Din Afefy, Pharos University, Egypt.
Reviewers:
(1) APACO JOAN, Kyambogo University, Uganda.
(2) Tayyab, The International University of Management, Namibia.
Complete Peer review History: https://www.sdiarticle4.com/review-history/73935

Original Research Article

Received 14 July 2021
Accepted 24 September 2021
Published 29 September 2021

ABSTRACT

Many researchers have been conducted on the ferrocement as a low cost construction material and a flexible structural system. This experimental investigation on the behavior of ferrocement beams after exposed to different type of ferrocement and different of ferrocement layer are presented in this paper. The experimental program consisted of seven simply supported beams tested up to failure under four-point load. The dimensions of 150mm×250mm×2000mm. Each beam was reinforced using steel 2 ϕ 12 in top and 2 ϕ10 in bottom and the stirrups was 10 ϕ 10/m. In addition to six of them contains ferrocement different steel wire meshes and different of ferrocement layer. The test specimens are divided in three groups and the results of each one compared with the control specimen. The first group (A) which used the welded wire mesh. The second group (B) which used the expanded wire mesh. But the third group (C) which reinforced using woven wire mesh. The mid span deflection, cracks, reinforcement and concrete strains of the tested beams were recorded and compared. The performance of the test beams in terms of ultimate flexure load cracking behavior and energy absorption were investigated. The experimental results emphasized that high ultimate loads, better crack resistance control, high ductility, and good energy absorption properties could be achieved by using the proposed ferrocement beams.

**Corresponding author: Email: abeermedhat1979@gmail.com;*

The cracks propagation decreased and its number and width decreased by using woven, expanded and welded wire mesh especially in specimens with two layers of wire mesh. Theoretical calculation was carried out to compare the oplained results with the theoretical ones, which show good agreement.

Keywords: Ferrocement beams; RC beams; steel mesh; ultimate load; cracking; ductility; energy absorption; welded wire mesh; expanded wire mesh; woven wire mesh.

1. INTRODUCTION

Ferrocement is a versatile construction material formed by using hydraulic cement mortar into closely spaced layers of a small sized wire mesh. The mesh may be of metallic or other materials. Ferrocement has a high tensile strength to weight ratio and better cracking resistance behavior when compared to reinforced concrete. Ferrocement may be defined as a thin wall reinforced concrete commonly constructed of hydraulic cement mortar reinforced with closely spaced layers of continuous and relatively small diameter wire mesh. Ferrocement is ideally suited for structures in which predominant membrane stresses occur. As a result, it has been extensively used to construct different element such as, tanks, roofs…etc. In the last few decades, incidence of failures of reinforced concrete structures has been seen widely because of increasing service loads and/or durability problems. The economic losses due to such failures are billions of dollars. Mansur and Paramasivan [1] carried out an experimental investigation in 1990 on ferrocement box-section short columns with and without concrete infill under axial and eccentric compression. The major parameters of the study were the types, arrangements, and volume fraction of reinforcement. Test results indicated that a ferrocement box- section can be used as a structural beams. Welded wire mesh has been found to perform better than an equivalent amount of woven mesh. In 1994, Kaushik et al. [2] carried out an investigation for ferrocement encased concrete columns. They have investigated short circular as well as square columns with unreinforced and reinforced cores. It was seen that the ferrocement encasement increases the strength and ductility of the columns for both axial and eccentric loading conditions. Another interesting research work was done by Ahmed et al. [3] to investigate the possibility of using ferrocement as a retrofit material for masonry columns. Uniaxial compression tests were performed on three uncoated brick columns, six coated brick columns with 25 mm plaster and another six columns coated with 25 mm thick layer of ferrocement. The study demonstrated that the use ferrocement coating strengthens brick columns significantly and improves their cracking resistance. Nedwell et al. [4] conducted a preliminary investigation into the repair of short square columns using ferrocement. Also, several investigations have reported on ferro-cement elements under axial load and eccentric compression [5-9]. Abdel Tawab [10] in 2006 investigated the use of U-shaped ferrocement permanent forms for the construction of beams and Hazem [11] in 2009, used non-metallic reinforcement for the U-shaped ferrocement forms instead of the conventional steel mesh. A short program was undertaken to provide some information regarding the effect of ferrocement repair on short columns subjected to axial loadings. It was found that the use of ferrocement retrofit coating increases the apparent stiffness of the columns and significantly improves the ultimate load carrying capacity. Overcrowded arrangement of rebars in reinforced concrete members, such as small beams, makes it difficult to compact concrete properly with the use of a mechanical vibrator. Self-compacting concrete (SCC) is a preferred substitution for conventional concrete where highly congested reinforcement is present or forms with complex shapes need to be filled. It is able to flow and consolidate under its own weight without the need for mechanical vibration (ACI 237R-07) [12]. The self-compacting concrete (SCC) was first developed by Okamura in 1986 [13,14]. Although widespread application of SCC is still hindered by a lack of manuals and codes, it is expected that SCC will gain more popularity globally as a cost saving option. There have been a number of notable studies on structural shear behavior and performanceof RC structures made with SCC [15-19].

2. EXPERIMENTAL PROGRAM

The experimental program was undertaken to investigate the general behaviour, cracks pattern, and the ultimate capacity of the reinforced

concrete rectangular beams reinforced using ferrocement composite. The experimental program consisted of seven composite beam section having the dimensions of 150 mm width, 250 mm depth and 2000 mm long span were cast and tested up to failure under four-point load. All specimens were reinforced with the same longitudinal bars in tension and compression of 2 ϕ 12 in bottom and 2 ϕ 10 in top and 10 ϕ 10/m for stirrups.

2.1 Characteristics of Materials

The concrete mix contents utilized for the experimental program was summarized in Table 1 which gives concrete characteristic strength of 30 MPa. The yield strength of the used reinforced steel was 360 MPa. The characteristics of used composite layers either expanded, welded and woven wire meshes were summarized in Table 2 and shown in Fig. 1. The beams were casted in a horizontal position and placed compacted in wooden molds.

Table 1. Concrete mixes, materials weights

Materials	Mix components F_{cu} = 30 MP_a
Silica fume	27.5 gm/m^3
Cement	550 Kg/m^3
Coarse aggregate	850 Kg/m^3
Fine aggregate	670 Kg/m^3
Water	200 L/m^3
Super-plasticizer	4.91 L/m^3

2.2 Preparation of Specimens and Samples Description

The experimental program consist of seven beams the first beam is control beam B01, having the same geometry and steel reinforcement details as shown in Fig. 1, were prepared for tested using four-point load. The control specimen was rectangular section beam reinforced using 2Ø12 in bottom and 2Ø10 in top and 10Ø10/m as stirrups along span of tested specimens. The group A consists of tow beams B02 and B03 which reinforced using one, two layers of welded wire mesh respectively. The group B for specimens B04 and B05 which reinforced using one, two layers of expanded wire meshes instead of stirrups respectively as described in Table 2. For group C of B06 and B07 which used one, two layers of woven wire meshes described in Table 2. The mechanical properties of the ferrocement composites used in the experimental program were given in Table 3 and its configuration in Fig. 2.

2.3 Test Setup

The tested beam sections were tested under two point load testing machine of maximum capacity of 600 KN with 1800 mm effective span and 500 mm for distance between two load as shown in Fig. 3. Load was affective at 20 KN increments on the tested specimens. The LVDT and dial gages were used of high accuracy to measure the deflections and strains for steel and concrete. The load still increased till failure load and maximum displacements.

Table 2. Specimens descriptions and notations

Group	Specimen ID.	Description of specimens	Reinforcement tension	Comp.	Reinforcement configuration
Control	B01	Control specimen	2 ϕ12	2 ϕ10	
A	B02	One layer welded wire mesh	2 ϕ12	2 ϕ10	
	B03	Two layer welded wire meshs	2 ϕ12	2 ϕ10	
B	B04	One layer expanded wire mesh	2 ϕ12	2 ϕ10	
	B05	Two layer expanded wire meshes	2 ϕ12	2 ϕ10	
C	B06	One layer woven wire mesh	2 ϕ12	2 ϕ10	
	B07	Two layer woven wire meshes	2 ϕ12	2 ϕ10	

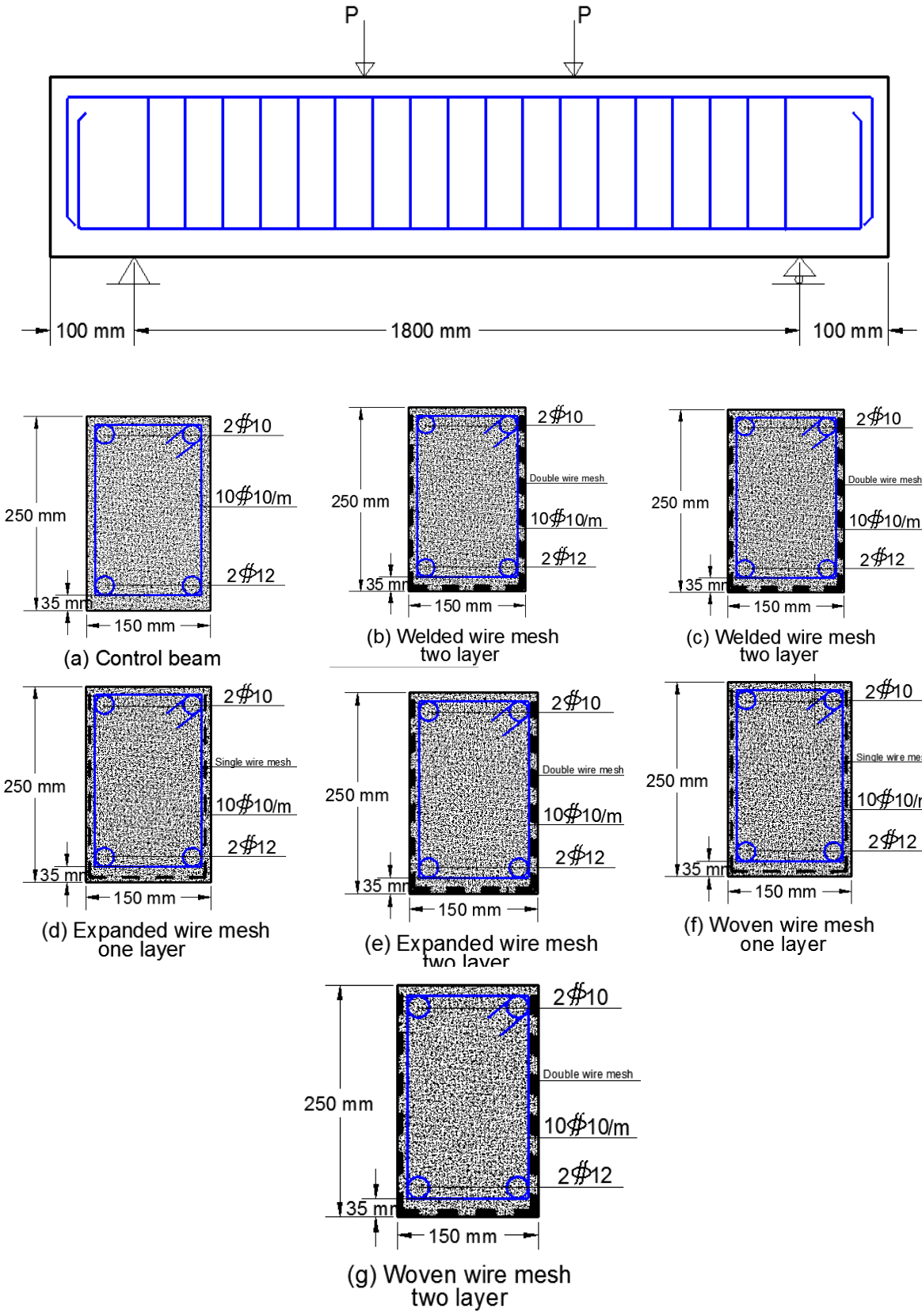

Fig. 1. Beams geometric shape and reinforcement details

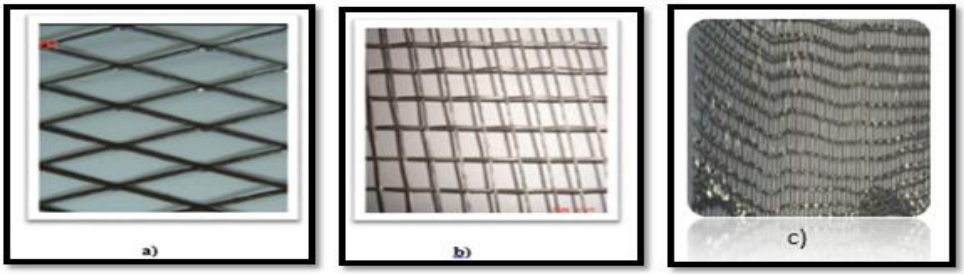

a) Expanded wire mesh, b) welded wire mesh; c) Woven wire mesh.

Fig. 2. Ferrocement composite

Table 3. Mechanical properties of expanded, welded and woven wire meshes

Mesh type	Tensile strength (MPa)	Youngs modulus (MPa)	Opens dimensions (mm)	Diameter (mm)
welded wire mesh	400	1700	10.0x10.0	0.7
Expanded wire mesh	250	1200	31.0x16.5	1.25
woven wire mesh	600	1500	4.0x4.0	2.0

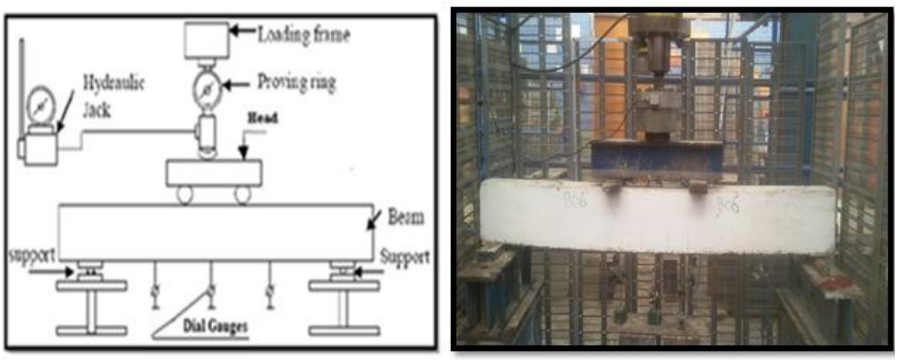

a) schematic shape b) photo of test set up

Fig. 3. Test Set up

3. TEST RESULTS AND DISCUSSION

Test results include the load carrying capacity and displacement in concrete beams. The cracks propagation during the tests was recorded. The crack initialization in the specimens reinforced using wire meshes was developed however, at later stages with respect to the control specimen. Besides, the cracks lengths and widths decreased in the specimens reinforced with either welded, expanded or woven wire mesh as compared to the control specimen.

3.1 Ultimate Failure Load and Deflection

The experimental failure loads for the control beam B01 and its corresponding deflection were recorded in Table 4 and Figs. 4, 5. The deflection was recorded using LVDT at the mid span verse to the corresponding experimental loads. It was observed that the load deflection curves for specimens reinforced using ferrocement composites was semi bilinear especially after reaching failure load, it decrease very rabidly. This behavior due to the failure mechanism of ferrocement and the type of concrete. For B01, the ultimate failure load was 64.0 KN with deflection of 47.0 mm.

For the group A which has concrete strength equals to 30 MPa and reinforcing using one layer and two layers of welded wire mesh of B02 and B03 respectively, the failure loads were 68.5 KN and 85.6 KN respectively. The deflections were

of 32.0 mm and 20.4 mm. the deflection decrease and the failure load increase due to high tensile strength of ferrocement layers composites with an enhancement ratios of 31.6% and 56.6% for B02 and B03 respectively as given in Table 4.

The group B which used expanded wire meshes, recorded failure loads of 64.31 KN and 71.0 KN for B04 and B05 respectively. The deflection of B04 was 30.0 mm but was 22.3 mm for B05 which used two layers of expanded wire meshes with an enhancement ratios of 36.1% and 52.3% for B04 and B05 respectively as given in Table 4.

For the group C which used woven wire mesh of high tensile strength and opens spaces with respect to the other wire meshes B06 and B07. The experimental failure loads were 78.5 KN and 89.0 KN respectively verse 24.4 mm and 20.3mm in deflection. This type of composite wires meshes show the most enhancement ratios in failure load capacity and deflection to be22.6% and 39.1% in carrying load capacity and 48.1% and 57.1% in deflections.These results indicating the good effect of using this type of ferrocement composites in ultimate carrying capacity and in deflection as in Fig. 6.

3.2 Mode of Failure

The mode of failure for the tested reinforced concrete beams were observed by naked eyes. This mode of failure was varied between flexural failures especially for beams reinforced using steel bars of B01. For specimens B02 to B07, the failure was tension failure which refer to the failure mechanism of ferrocement composites. This was as the previous studied [4,5] recorded similar mode of failure in specimens reinforced by ferrocement composites.

Near failure, the control specimen failed in a mode of tension failure accompanied with local crushing and spalling of the concrete in the surface of the beams. For the other series of the tested specimens, near failure the load reach the maximum value and after this value the load decreased up to 70% to 50% of the maximum load with increasing the descending part of load displacement curves. This increases the ductile behaviour and the energy absorption of these specimens as shown in Table 5.

3.3 Volume Fraction of Steel Reinforcement

Experimental results revealed that, increasing of the volume fraction of steel reinforcement contributed to relatively higher ultimate load. This is clear when comparing beam B01 and the other beams which showing the different degrees of increasing in the ultimate failure load, and enhancing many properties.

3.4 Ductility and Energy Absorption

Ductility is defined as the ratio between the deformations at first crack ultimate load to the deformation at the ultimate load, while the energy absorption is the total area under the load deflection curve. Table 5 the energy absorption and the ductility ratio for all tested beams. A progressive increase of energy absorption with volume fraction percentage and ductility was observed. For the control specimen, the energy absorption was recorded to be 1504.0 KN.mm. Comparing this value with the recorded values for different groups showed large increase in the energy absorption capacity for all specimens.

Table 4. Comparison between failure loads of test specimens

Group	Specimen ID.	Failure load (KN)	Ultimate deflection (mm)	% of enhancement $(\frac{Pu - Pucontrol}{Pucontrol})$	% of deflection enhancement $(\frac{\Delta u - \Delta ucontrol}{\Delta ucontrol})$
Control	B01	64.0	47.0	------	-----
A	B02	68.5	32.0	7.03	31.9
	B03	85.6	20.4	33.75	56.6
B	B04	64.3	30.0	0.47	36.1
	B05	71.0	22.3	11.09	52.3
C	B06	78.5	24.4	22.6	48.1
	B07	89.0	20.3	39.10	57.1

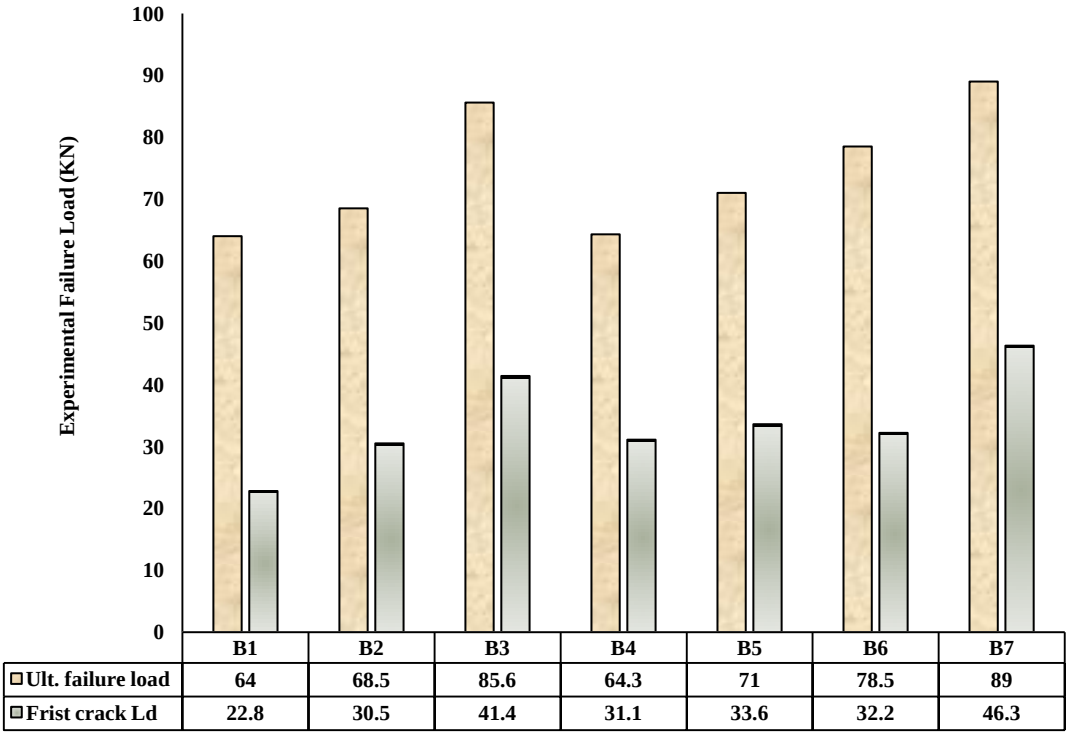

	B1	B2	B3	B4	B5	B6	B7
Ult. failure load	64	68.5	85.6	64.3	71	78.5	89
Frist crack Ld	22.8	30.5	41.4	31.1	33.6	32.2	46.3

Fig. 4. Comparisons between Experimental Failure Loads.

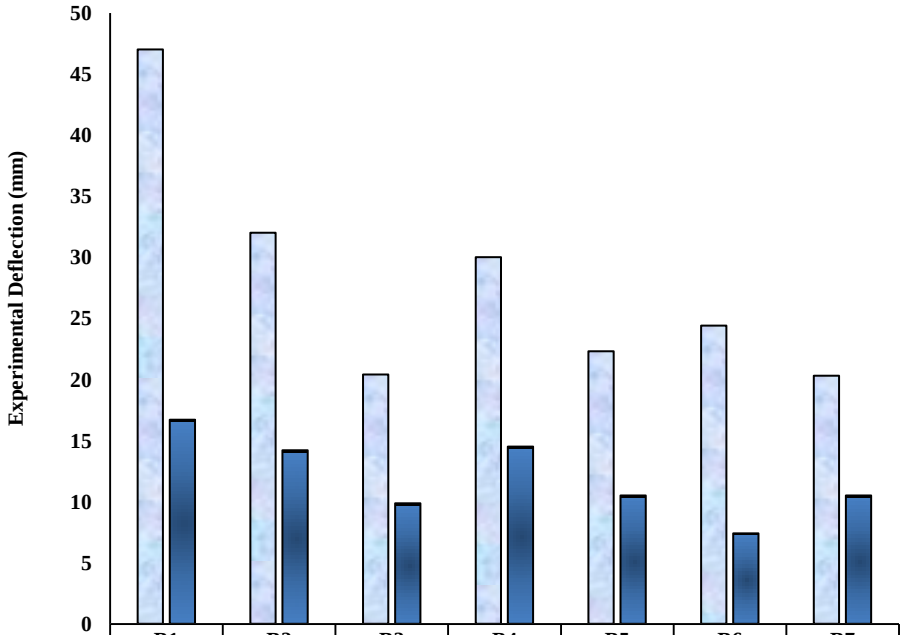

	B1	B2	B3	B4	B5	B6	B7
Ult. deflection	47	32	20.4	30	22.3	24.4	20.3
Frist crack def.	16.7	14.2	9.86	14.5	10.5	7.4	10.5

Fig. 5. Comparisons between experimental deflections

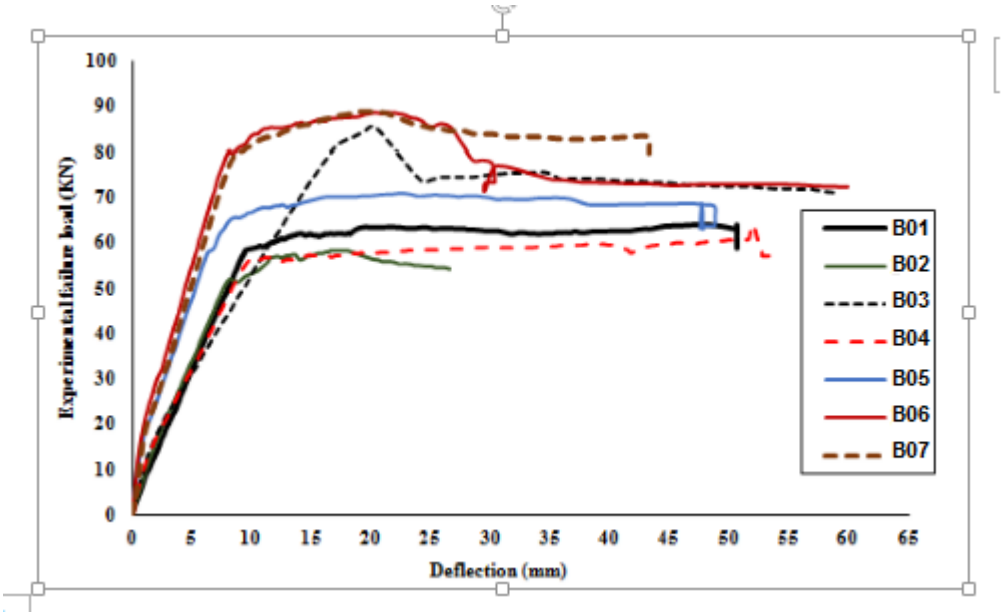

Fig. 6. Load deflection curves of tested beams

Table 5. Comparison between experimental results

Group	Specimen ID.	Frist crack load (KN)	Ultimate Failure load (KN)	Ductility (%)	Energy absorption (KN.mm)
Control	B01	22.8	64.0	35.6	1504.0
A	B02	30.5	68.5	44.5	1096
	B03	41.4	85.6	48.4	873.12
B	B04	31.1	64.3	48.3	964.5
	B05	33.6	71.0	47.3	791.65
C	B06	32.2	88.5	36.4	902.7
	B07	46.3	89.0	52.0	903.7

For the ductility ratio obtained for the control specimen was 36.6%. A progressive increase in ductility obtained for different groups of specimens. For series A, the ductility varied between 44.5% and 48.4% for B02 and B03. For series B and C the ductility varied between 36.0% to 52.0%. This shows the enhancement in ductility in beams using ferrocement layers.

Finally using these innovative composite materials enhanced the behavior of the tested beams. It can be state that it delayed the appearance of the first cracks and increased the service load capacity. In addition, it developed with high ultimate loads, crack resistance, better deformation characteristics, high durability, high ductility and energy absorption properties, which are very useful for dynamic applications.

3.5 Cracking Propagation

The control specimen B01 which reinforcing using 2ϕ12 as tension steel and 2ϕ10 as compression steel with 10ϕ10/m steel stirrups, the cracks were notice by eye. The first crack in this specimen started at load of 23.6 KN developed under the load point in the mid span as shown in Fig. 5 and Table 5.

For specimen B02 & B03 which reinforced using 2ϕ12 as tension steel and 2ϕ10 as compression steel without stirrups. The one layer and two layers welded wire meshes were used instead of stirrups respectively. The recorded first crack load noticed were 30.4 KN and 41.4 KN for B02 and B03 respectively. This showed an enhancement about 33.7% and 81.6% respectively.

For specimen B04 & B05 which reinforced using 2ϕ12 as tension steel and 2ϕ10 as compression steel without stirrups. The one layer and two layers expanded wire meshes were used instead of stirrups respectively. The recorded first crack load noticed were 31.1 KN and 33.6 KN for B04

and B05 respectively. This showed an enhancement about 36.4% and 47.4% respectively.

For specimen B06 & B07 which reinforced using 2ϕ12 as tension steel and 2ϕ10 as compression steel without stirrups. The one layer and two layers woven wire meshes were used instead of stirrups respectively. The recorded first crack load noticed were 32.2 KN and 46.3 KN for B06 and B07 respectively. This showed an enhancement about 41.2% and 103.1% respectively showing high enhancement in cracks.

Generally, the cracks for all tested beams started at later stage of loading and started to increase in number and length till failure, indicating better confinement and better serviceability. However, different types of innovative composite the ultimate strength increased and the cracks slightly increased in length and width to different extent. As shown in Fig. 7 to Fig. 10 and Table 5.

Fig. 7. Crack pattern of control beam B01

a)

b)

Fig. 8. Crack Pattern of Group A, a) Beam B02; b) Beam B03

a)

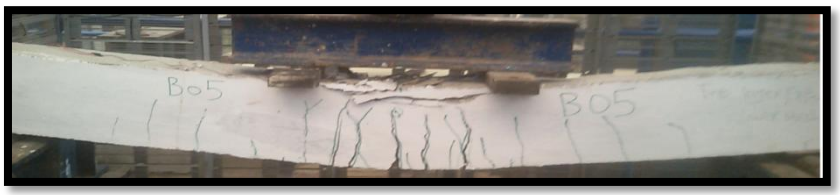

b)

Fig. 9. Crack Pattern of Group B, a) Beam B04; b) Beam B05.

a)

b)

Fig. 10. Crack Pattern of Group C, a) Beam B06; b) Beam B07.

3.6 Theoretical Calculation of Ultimate Flexural Load

To increase the flexural strength, the ferrocement laminates are attached to the tension side of the reinforced concrete beams. The theoretical method used in this research to compute the ultimate load for the test specimens is similar to that presented by Abdel Tawab (2006). The following assumptions are made in calculating the ultimate moment capacity of the beam.

- The strain in reinforcement and concrete is directly proportional to the distance from the neutral axis.
- The plane sections before loading remain plane and after loading.
- There is no relative slip between ferrocement laminate and the concrete.
- Failure occurs when the maximum compressive strain in the form's beam matrix and the concrete core reaches 0.0035.
- At ultimate load, the tensile contribution of beam matrix and the concrete core are neglected and the compressive contribution is represented by a rectangular stress block of depth (a) equals to 0.8dn and stress of 0.67fcu.
- The maximum compressive strain in concrete is 0.0035 in bending.
- The tensile strength of concrete is neglected.
- The mesh reinforcement in ferrocement laminate has linear elastic stress strain relationship to failure.
- Shear deformation is small.

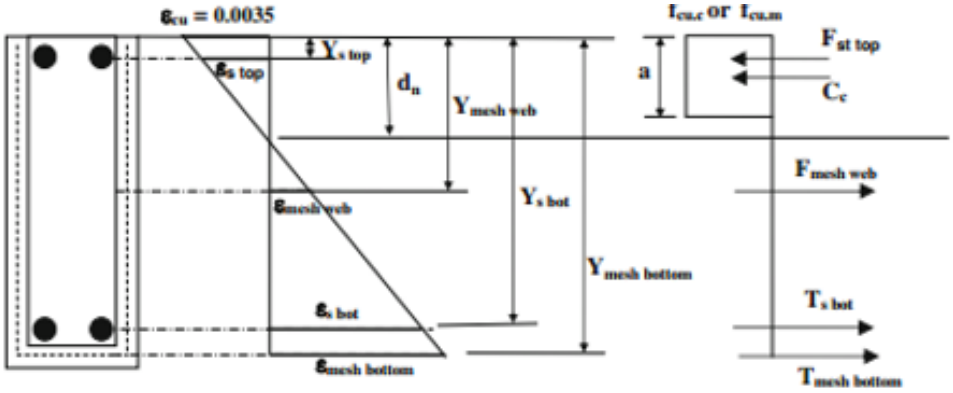

Fig. 11. Theoretical strain and Stress distribution and internal forces on the cross section

(Fs.top + Fmesh.web + Ts bot + T mesh.bot- Cc) = 0 (1)

The internal forces Cc, Fs.top, Fmesh.web, Ts.bot, and Tmesh.bot are shown in Fig. 11 and are given by:

- Cc = ab fcu.c (2)
- Fs.top = ϭs.topAs.top (3)
- Fmesh.web = ϭ mesh.web(2A mesh.web)(4)
- Ts bot = ϭs.botAs.bot (5)
- T mesh.bot = ϭ mesh.bot A mesh.bot (6)
- ϭs.bot = EsƐs.bot≤ Fys (if Ɛs.bot ≤ Ɛys) (7)
- ϭs.bot = Fys + Esth (Ɛs.bot - Ɛys) ≤ Fus (if Ɛs.bot > Ɛys) (8)
- ϭs.top = EsƐs.top≤ Fys (if Ɛs.top ≤ Ɛys) (9)
- ϭs.top = Fys + Esth (Ɛs.top - Ɛys) ≤ Fus (if Ɛs.top > Ɛys) (10)
- ϭ mesh .web = EsƐ mesh .web ≤ Fym (11)
- ϭ mesh .bot = EsƐ mesh .bot ≤ Fym (12)

The strain at the top steel bars, bottom steel bars, web steel meshes, and bottom steel meshes could be obtained from the geometry of the strain distribution shown in Fig. 11. ϭs.top and Ɛ mesh .web could be tension (positive sign) or compression (negative sign) depending on the location of the neutral axis. The location of the neutral axis (X) is determined by applying trial and error method until Eq. (1) is satisfied. The calculation was performed on the computer using the Microsoft EXCEL sheet. Once the location of the neutral axis is determined and the internal forces are determined, the ultimate moment on the section (Mu) can be calculated by taking the moment about the point of application of the compression force as follows:

Mu = Ts.bot Ys.bot + Fs.top Ys.top + Fmesh.web Ymesh.web + Fmesh.bot Ymesh.bot (13)

Accordingly, for simply supported beam subjected to central concentrated load, the ultimate load (Pu1) is obtained from the following formula:

Mu = Pu*L/4 (14)

List of Symbols:

As. bot : Area of the steel bars at bottom of the beam.
As. top: Area of the steel bars at top of the beam (if they exist).
A mesh.bot : Area of the steel meshes in the beam layer under the core.
A mesh.web: The cross sectional area of the web mesh reinforcement in the vertical direction within a length equal to (d)
a: Depth of the compression block
b : Total width of the beam
Cc : The compressive force on the concrete block
d : The depth of the beam
dn : Neutral axis depth from the top of the specimen
Es : Modulus of elasticity of the steel
Fmesh.web: The force on the mesh reinforcement in the two faces of the beam which could be positive or negative depending on the location of the neutral axis.
Fs.top: The force on the top reinforcement which Could be positive or negative depending on the location of the neutral axis.
Fys, Fym : Yield stress or proof stress of the reinforcing steel bars and steel mesh
fcu.c: Compressive strength of the concrete.
Mu: Ultimate moment of the beam
Pu : Ultimate load for flexural failure
Tmesh.bot : The tensile force on the steel mesh at the bottom of the beam
Ts.bot: The tension force on the bottom steel
ys.bot : Distance between the bottom steel bars and the compressive force (Cc)
ys.top: Distance between the top steel bars and the compressive force (Cc)
ymesh.web: Distance between the center of the web steel mesh and the compressive force (Cc)
ymesh.bot: Distance between the bottom steel meshes and the compressive force (Cc)
Esth : Strain-hardening modulus of the steel
Ɛys : Yield strain of the reinforcing steel bars
Ɛmesh.web, ϭ mesh.web: Strain and stress at the level of mesh reinforcement at the sides of the beam
Ɛmesh.bot, ϭ mesh.bot: Strain and stress at the level of mesh reinforcement at the bottom of the beam
Ɛs.bot, ϭ s.bot : Strain and stress at the level of bottom steel bars
Ɛs.top, ϭ s.top : Strain and stress at the level of top steel bars.

Table 6. Theoretical first crack and ultimate loads and comparison with experimental results

Number	Distance to neutral axis from top of beam (mm)	Theoretical Moment (Mu.theor) (KN.M)	Theoretical load (Pu.theor) (kN)	Tested ultimate load Pu (kN)	Pu.exp/Pu.theor
B01	8.25	23.98	73.78	64	0.87
B02	34.70	29.42	90.54	68.5	0.76
B03	61.16	40.76	125.40	85.6	0.68
B04	35.59	29.84	91.81	64.3	0.70
B05	62.92	41.44	127.25	71.1	0.56
B06	70.11	44.11	135.73	88.5	0.65
B07	131.97	60.71	186.79	101.5	0.54

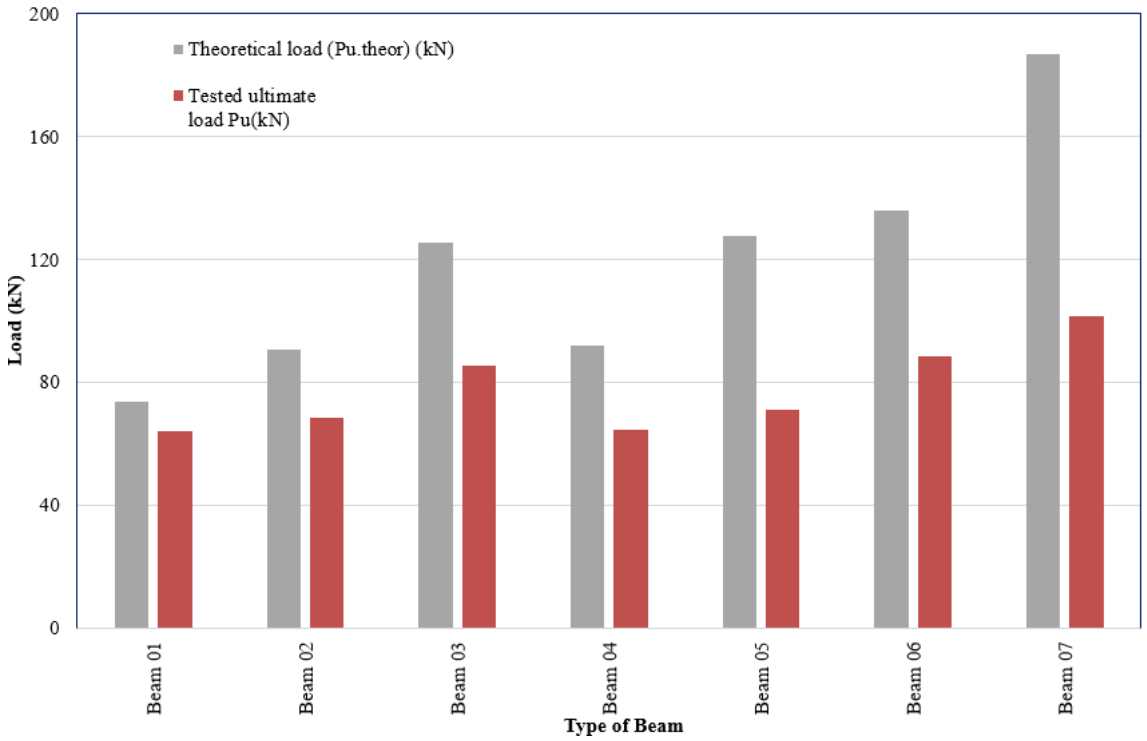

Fig. 12.Theoretical strain and stress distribution and internal forces on the cross section.

4. CONCLUSIONS

Based on the results and observations of the experimental study presented in this thesis and considering the relatively high variability and the statistical pattern of data, the following conclusions can be drawn:

1- Welded, expanded and woven wire meshes exhibited features over normal reinforcement with reinforcing steel, epically in rectangular beams such that, it has normal strength, easy to be handling cutting and shaped also has light weight.

2- The test results show that the woven wire mesh exhibited a higher ultimate load than Conventionally reinforced control beams by about 39.1%.

3- Woven wire mesh has high effect in increasing load capacity, deflection, the flexural stresses and cracks propagate.

4- The cracks propagation decreased and its number and width decreased by using woven, expanded and welded wire mesh especially in specimens with two layers of wire mesh.

5- Experimental results revealed that increasing the volume fraction of steel reinforcement contributed to a slightly higher ultimate load and higher energy absorption.

6- Therefore increasing volume fraction percentage has a dominant effect in delaying occurrence of the developed cracks with high protection against corrosion and high strength gain compared with those reinforced with metallic reinforcement.

COMPETING INTERESTS

Authors have declared that no competing interests exist.

REFERENCES

1. Mansur MN, Paramasivam P. Ferro-cement short columns under axial and eccentric compression. ACI structural Journal. 1990;84(5):523.
2. Kaushik SK, Prakash A, Singh KK. Inelastic buckling of ferro-cement encased columns. In Proceedings of the Fifth International Symposium on Ferrcement, Nedwell and Swamy (eds), London: E& FN Spon. 1994;327-341.
3. Ahmed T, Ali SKS, Choudhury JR. Experimental study of ferro-cement as a retrofit material for masonry columns. In Proceedings of the Fifth International Symposium on Ferrcement, Nedwell and Swamy (eds), London: E& FN Spon. 1994;269-276.
4. Nedwell PJ, Ramesht MH, Rafei-Taghanaki S. Investigation into the repair of short square columns using ferro-cement. In Proceedings of the Fifth International Symposium on Ferrcement, Nedwell and Swamy (eds), London: E& FN Spon. 1994;277-285.
5. Fahmy E, Shaheen YB, Korany Y. Repairing reinforced concrete columns using ferro-cement laminates. Journal of ferro-cement. 1999;29(2):115-124.
6. Fahmy EH, Shaheen YBI, Korany YS. Environmentally friendly high strength concrete. Proceedings of the 24th Conference on Our World in Concrete and Structures. 1999;171-178.
7. Fahmy EH, Shaheen YB, Abou Zeid MN, Gaafar H. Ferro-cement sandwich and cored panels for floor and wall construction. Proceedings of the 29th Conference on Our World in Concrete and Structures. 2004;245-252.
8. Fahmy EH, Shaheen YB, Abou Zeid MN. Development of Ferro-cement Panels for Floor and Wall construction. 5th Structural Specialty Conference of the Canadian Society for Civil Engineering, ST218-1-ST218-10; 2004.
9. Fahmy EH, Abou Zeid MN, Shaheen YB, Gaafar H. Behavior of ferro-cement panels under axial and flexural loadings. Proceedings of the 33rd Annual General Conference of the Canadian Society of Civil Engineering, GC-150-1-GC-150-10; 2005.
10. Abdel Tawab, Alaa, Development of permanent formwork for beams using ferro-cement laminates. P.H.D. Thesis, submitted to Menoufia University, Egypt; 2006.
11. Hazem R. Non-metallic Reinforcement for the U-shaped ferro-cement forms instead of the conventional steel mesh. Deutsches Zentrum für Entwicklungstechnologien; 2009.Retrieved on February 20.
12. ACI Committee 237. “Self-consolidating concrete,” ACI 237R-07, ACI Committee 237Report, American Concrete Institute, Farmington Hills, Michigan. 2007;32.
13. Choulli Y, Marı´ AR, Cladera A. Shear behavior of full-scale prestressed I-beams made with self compacting concrete,” Materials and Structures. 2008;41:131-141.
14. Hassan AAA, Hossain KMA, Lachemi M. Behavior of fullscale self-consolidating concrete beams in shear. Cement and Concrete Composites. 2008;30:588-596.
15. Hassan AAA, Hossain KMA, Lachemi M., Structural assessment of corroded self-consolidating concrete beams. Engineering Structures. 2010;32:874-885.
16. Lachemi M, Hassain KMA, Lambros V, Nkinamubanzi PC, Bouzoubaa N. Self-compacting concrete in corporating new viscosity modifying admixtures. Cement and Concrete Research. 2005;24:917-926.
17. Hassan SA. Behavior of reinforced concrete deep beams using self compacting concrete. PhD Thesis, University of Baghdad, Civil Department, Baghdad, Iraq. 2012;164.
18. Mahmoud KSh. Experimental study of the shear behavior of self compacted concrete

T-beams, Journal of Engineering and Development. 2012;16(1).

19. Fahmy Yousry BI, Shaheen Ezzat H, Ahmed Mahdy Abdelnaby, Mohamed N Abou Zeid. Applying the ferro-cement concept in construction of concrete beams incorporating reinforced mortar permanent forms. International Journal of Concrete Structures and Materials. 2013;27.

Peer-review history:
The peer review history for this paper can be accessed here:
https://www.sdiarticle4.com/review-history/73935